Journal Pre-proofs

Optimization of globomycin analogs as novel gram-negative antibiotics

Keira Garland, Homer Pantua, Marie-Gabrielle Braun, Daniel J. Burdick, Georgette M. Castanedo, Yi-Chen Chen, Yun-Xing Cheng, Jonathan Cheong, Blake Daniels, Gauri Deshmukh, Yuhong Fu, Paul Gibbons, Susan L. Gloor, Rongbao Hua, Sharada Labadie, Xiongcai Liu, Richard Pastor, Craig Stivala, Min Xu, Yiming Xu, Hao Zheng, Sharookh B. Kapadia, Emily J. Hanan

PII: S0960-894X(20)30530-8
DOI: https://doi.org/10.1016/j.bmcl.2020.127419
Reference: BMCL 127419

To appear in: *Bioorganic & Medicinal Chemistry Letters*

Received Date: 8 June 2020
Revised Date: 13 July 2020
Accepted Date: 14 July 2020

Please cite this article as: Garland, K., Pantua, H., Braun, M-G., Burdick, D.J., Castanedo, G.M., Chen, Y-C., Cheng, Y-X., Cheong, J., Daniels, B., Deshmukh, G., Fu, Y., Gibbons, P., Gloor, S.L., Hua, R., Labadie, S., Liu, X., Pastor, R., Stivala, C., Xu, M., Xu, Y., Zheng, H., Kapadia, S.B., Hanan, E.J., Optimization of globomycin analogs as novel gram-negative antibiotics, *Bioorganic & Medicinal Chemistry Letters* (2020), doi: https://doi.org/10.1016/j.bmcl.2020.127419

Journal Pre-proofs

Bioorganic & Medicinal Chemistry Letters
journal homepage: www.elsevier.com

Optimization of globomycin analogs as novel gram-negative antibiotics

Keira Garland,[a,†] Homer Pantua,[a] Marie-Gabrielle Braun,[a] Daniel J. Burdick,[a] Georgette M. Castanedo,[a] Yi-Chen Chen,[a] Yun-Xing Cheng,[b] Jonathan Cheong,[a] Blake Daniels,[a,‡] Gauri Deshmukh,[a] Yuhong Fu,[b] Paul Gibbons,[a,§] Susan L. Gloor,[a,□] Rongbao Hua,[b] Sharada Labadie,[a] Xiongcai Liu,[b] Richard Pastor,[a] Craig Stivala,[a] Min Xu,[a] Yiming Xu,[a] Hao Zheng,[a] Sharookh B. Kapadia,[a] and Emily J. Hanan,[a*]

[a]*Genentech, Inc., 1 DNA Way, South San Francisco, CA, 94080, USA*
[b]*Pharmaron Beijing Co., Ltd, No. 6 Taihe Road, BDA, Beijing, 100176, P.R. China*

ARTICLE INFO

Article history:
Received
Revised
Accepted
Available online

Keywords:
Signal peptidase
LspA
Globomycin
Gram-negative

ABSTRACT

Discovery of novel classes of Gram-negative antibiotics with activity against multi-drug resistant infections is a critical unmet need. As an essential member of the lipoprotein biosynthetic pathway, lipoprotein signal peptidase II (LspA) is an attractive target for antibacterial drug discovery, with the natural product inhibitor globomycin offering a modestly-active starting point. Informed by structure-based design, the globomycin depsipeptide was optimized to improve activity against *E. coli*. Backbone modifications, together with adjustment of physicochemical properties, afforded potent compounds with good in vivo pharmacokinetic profiles. Optimized compounds such as **51** (*E. coli* MIC 3.1 μM) and **61** (*E. coli* MIC 0.78 μM) demonstrate broad spectrum activity against gram-negative pathogens and may provide opportunities for future antibiotic discovery.

* Corresponding author. Tel.: +1-650-225-4577; e-mail: hanan.emily@gene.com
Present Address: †Proneurotech, ‡Wilson Sonsini Goodrich & Rosati, §ORIC Pharmaceuticals, □EpiCypher, Inc.

M that bacteria remain a significant medical challenge and there is an urgent need for new classes of antibiotics to address the emerging resistance to the current classes of antibiotics.[1] Despite this clinical need, there have been no new approved classes of antibiotic for Gram-negative pathogens in over fifty years. The lipoprotein biosynthetic pathway presents a compelling opportunity for antibacterial discovery, with multiple enzymes located in the inner membrane that are required for the post-translational processing of lipoproteins.[2,3] Lipoprotein signal peptidase II (LspA) is responsible for cleaving the signal peptides from diacylated prolipoproteins to enable their subsequent modification and trafficking to the outer membrane (OM), and is essential for growth in all clinically relevant Gram-negative bacteria.[4] Inhibition of LspA in wild-type *Escherichia coli* results in mis-localization and accumulation of peptidoglycan-linked Braun's lipoprotein (Lpp) in the inner membrane leading to bacterial cell death.[4-6]

Two natural products are known to selectively inhibit LspA: globomycin, produced by *Streptomyces* species, and myxovirescin, produced by *myxobacteria* (Figure 1).[7-10] Although non-natural product derived inhibitors of LspA have been reported, they lack measurable growth inhibition against wild-type Gram-negative bacteria.[11] Globomycin, a cyclic depsipeptide, has previously been optimized with some improvement in activity against *Enterobacteriaceae.* However, these analogs still lacked activity against non-fermenter species such as *Acinetobacter* and *Pseudomonas* species.[12,13] Additionally, all analogs retained a metabolically labile ester moiety, and hence were unsuitable for in vivo evaluation. The 2016 publication of a co-crystal structure of globomycin with LspA offered new opportunities for structure-based drug design and further optimization of the globomycin scaffold.[14]

Figure 1. Natural product inhibitors of LspA

As described by Vogeley et al., globomycin occupies the putative active site of LspA and forms both polar and hydrophobic interactions with the protein.[14] The peptide backbone of globomycin engages in the majority of the polar interactions in the center of the binding site, with the lipophilic side chains and *n*-hexyl tail nestled against the membrane-facing surface of the protein. While we sought to optimize these interactions, we also sought to improve permeation of these molecules through the OM. The mechanism by which globomycin penetrates the OM is not entirely clear: its size likely precludes it from transversing through general porins, and the significant difference in minimum inhibitory concentration (MIC) against wild-type and a membrane permeabilized *E. coli* strain are consistent with the OM permeability barrier of Gram-negative bacteria limiting globomycin penetrance.[15] In addition, with a 39-fold improvement in MIC when tested in an *E. coli* efflux pump (*tolC*) mutant strain (Table S1), gobomycin appears to be a substrate of the TolC efflux pump, which likely plays a role in limiting its intracellular concentration. However, interpreting the magnitude of efflux liability using the *tolC* strain is complicated by the impact on OM integrity with the loss of the TolC protein.

To inform our SAR studies, we measured MICs in both the wild-type uropathogenic clinical *E. coli* isolate (CFT073) and an OM-permeable mutant of CFT073 (CFT073*imp*4213). Differences in activity between these two strains can elucidate how changes to an inhibitor affects its ability to penetrate the outer membrane of the bacteria, vs. its ability to bind to the target protein. To avoid optimization of cell killing via off-target activity or general membrane disruption, we also monitored activity against the Gram-positive *Staphylococcus aureus* (*S. aureus*) *S. aureus* strains with defective lipoprotein biosynthesis are viable in vitro.[16] Globomycin itself shows no activity against S. aureus up to 100 μM.

Both solution-phase and solid-phase syntheses of the globomycin scaffold have been previously reported.[17,18] We first synthesized the lipophilic tail fragments utilizing the Oppolzer's sultam chiral auxiliary to generate the chiral aldol product, with auxiliary cleavage providing the chiral carboxylic acids **A1** and **A2** (Scheme 1).[19] We synthesized the peptide backbone utilizing standard solid-phase synthesis techniques, and triphosgene to facilitate the final coupling between **A1** or **A2** and the hindered *N*-methyl peptide.[20] After cleavage from resin, macrocyclization of the linear peptide was effected under Shiina lactonization[21] conditions, and subsequent global deprotection of amino acid side chains afforded the final products (Scheme 2).

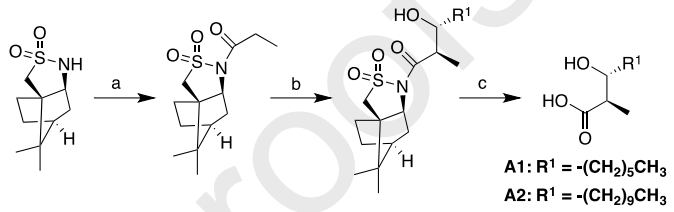

Scheme 1. Reagents and conditions: (a) propionyl chloride, triethylamine, 4-dimethylaminopyridine, THF; (b) R^1-CHO, CaH_2, TBDMSOTf, Et_3N, $TiCl_4$, DCM, 0 °C-r.t.; (c) LiOH or $KOSi(CH_3)_3$, H_2O, THF

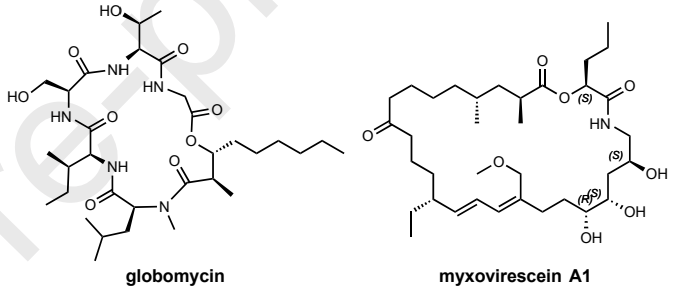

The SAR described by Kiho et al. indicated a correlation between increasing potency and extension of the linear aliphatic tail and no change in potency when inverting the side chain stereochemistry of the *allo*-isoleucine residue to an isoleucine. We were able to recapitulate these results with globomycin and compounds **1** and **2** (Table 1). We were particularly interested in modifying the serine residue based on observations in the co-crystal structure of globomycin and LspA, in which the sidechain hydroxyl appears to form a bridging hydrogen bond between the two putative catalytic aspartate residues in the active site.[14]

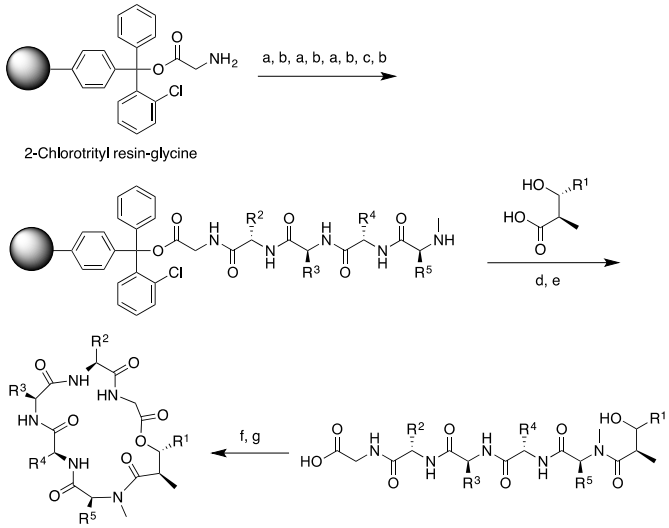

Mo[illegible]ngth complete loss of activity confirmed the importance of this residue. We hypothesized that changing this hydroxyl to a positively charged moiety would enable a stronger salt-bridge interaction. A variety of positively charged side chains (compounds **4**-**7**) were evaluated and the 2,3-diaminopropionic (Dap) residue (**4**) was found to provide the best activity. Interestingly, in the context of the *n*-decyl tail, the improvement in activity was observed only in the WT strain (compound **4** vs **2**), while in the context of the *n*-hexyl tail both OM-permeabilized and WT MICs were improved by 5-fold (**8** vs globomycin).

Scheme 2. Reagents and conditions: (a) *N*-Fmoc protected amino acid, HOBt, DIPEA, DMF; (b) 20% piperidine in DMF; (c) *N*-methyl-*N*-Fmoc protected amino acid, HOBt, DIPEA, DMF; (d) triphosgene, DIPEA, collidene, THF; (e) 7:2:1 DCM:AcOH:TFE; (f) 2-methyl-6-nitrobenzoic anhydride, 4-dimethylaminopyridine, THF/DCM; (g) global deprotection: TFA or Pd-C/H_2/EtOAc.

Adjacent to the serine, the *allo*-isoleucine residue makes hydrophobic contacts with the protein. As illustrated in Table 1, we elucidated several trends at this position: preference for branching location in alkyl chains (*allo*-isoleucine **8** vs leucine **9**), increased activity for aliphatic over aromatic side chains (**10** and **11**), and enhanced potency for cyclic aliphatic groups such as cyclohexyl and cycloheptyl glycine (**12** and **13**). While this side chain does reach the edge of the active site, it is expected that this region of the protein is not solvent facing, but buried within the inner membrane. Consistent with the highly lipophilic environment, polar side chains at this position, either with or without hydrogen bond donors, completely ablated activity (e.g., compounds **14** - **16**). The next residue in the globomycin scaffold, *N*-methyl-leucine, is in a similarly lipophilic environment, and we again found that polar side chains were not tolerated (Supplemental Table S2). Branching was also not required and small aliphatic side chains such as norvaline retained activity (compound **17**), although further reduction in side chain length (e.g. ethylglycine **18**) reduced activity (Table 1).

The lipid tail of globomycin appears to make favorable hydrophobic interactions along a shallow groove in the surface of the protein adjacent to the active site. As was shown by Kiho and [illegible] of this tail from C6 to C10 enhances potency. However, as shown in Supplemental Table S2, many compounds with a C10 tail begin to show apparent off-target activity against the gram-positive pathogen *S. aureus* USA300. Activity against *S. aureus* USA300 roughly correlates with lipophilicity, particularly for compounds with LogD > 4.0, suggesting the influence of a non-specific mechanism of action which prompted us to evaluate alternatives to a linear aliphatic tail (Table 2). The corresponding chiral carboxylic acids were prepared following methods analogous to those described in Scheme 1 (see Supplementary Material for details). Both terminal and interior branching was tolerated with **20** and **21** providing similar potency to **19** and with reduced *S. aureus* USA300 activity. A terminal CF_3 group (**22**) as well as mono-fluorinated compound **23** showed significantly reduced activity in both OM-permeabilized and wild-type *E. coli* relative to **12**. The introduction of polar heteroatoms, such as ethers, sulfones, or amines, typically ablated all activity (Supplemental Table S3). Compounds **24** and **25** with a tertiary alcohol or ether (Table 2) were exceptions that retained some activity; the latter ether **25** was equipotent to compound **19** but with a reduced LogD. Extension of the methyl group adjacent to the lipophilic tail was tolerated as long as a combined minimum number of carbons was maintained, but no significant improvements in potency were found and lipophilicity was generally increased (Supplemental Table S4). An attempt to reduce the conformational flexibility of the hydrophobic tail led to compounds **26**-**29** shown in Table 3. As compared to compound **13** (LogD 3.4, *S. aureus* USA300 MIC 50 μM), these compounds afforded good activity, reaching sub-μM MICs with reduced lipophilicity. Norbornyl analogs **26** (exo) and **27** (endo) also demonstrated reduced *S. aureus* USA300 activity relative to **13**. The tolerance for lipophilic groups with a variety of constrained 3D character is consistent with non-specific hydrophobic interactions at the interface of the protein and the interior of the inner membrane.

In order to progress LspA inhibitors towards in vivo studies, we profiled the pharmacokinetics of globomycin itself both in vitro and in vivo. It was found to be labile in mouse plasma (49% remaining after 6 hour incubation), presumed to be the result of esterase activity. Existing SAR indicated that the corresponding amide to the globomycin ester has no measurable activity.[13]

Table 1. Globomycin analogs[a]

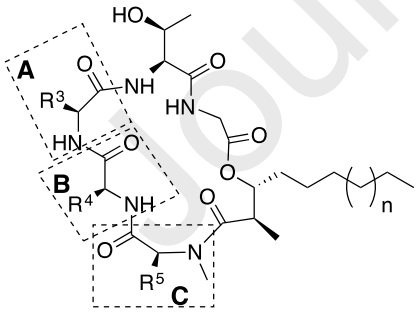

Compound	A	B	C	n	CFT073*imp*4213[b] MIC (μM)	CFT073[b] MIC (μM)	USA300[c] MIC (μM)
globomycin	Ser	*allo*Ile	Leu	1	0.25	44	>100
1	Ser	*allo*Ile	Leu	5	0.016	5.4	25
2	Ser	Ile	Leu	5	0.016	9.4	25
3	Ala	Ile	Leu	5	25	100	25
4	Dap	Ile	Leu	5	0.03	2.2	13

5							
6	His	Ile	Leu	5	6.3	100	25
7	Agp	Ile	Leu	5	1.6	50	13
8	Dap	*allo*Ile	Leu	1	0.053	8.6	>100
9	Dap	Leu	Leu	1	0.4	25	>100
10	Dap	Phe	Leu	1	0.8	50	>100
11	Dap	Phg	Leu	1	1.6	71	>100
12	Dap	Chg	Leu	1	0.059	3.1	>100
13	Dap	C7g	Leu	1	0.014	1.1	50
14	Dap	Thr	Leu	1	50	>100	>100
15	Dap	Thr(Me)	Leu	1	7.7	>100	>100
16	Dap	Gln	Leu	1	>100	>100	>100
17	Dap	Chg	Nva	1	0.049	3.5	>100
18	Dap	Chg	Abu	1	0.14	8.8	>100

[a]Agp = (S)-2-amino-3-guanidinopropanoic acid; Dap = (S)-2,3-diaminopropionic acid; Dab = (S)-2,3-diaminobutyric acid; Phg = phenylglycine; Chg = cyclohexylglycine, C7g = cycloheptylglycine, Thr(Me) = O-Methyl-L-threonine, Nva = norvaline; Abu = aminobutyric acid; [b] *E. coli;* [c] *S. aureus*

Table 2. Effects of hydrophobic tail modification

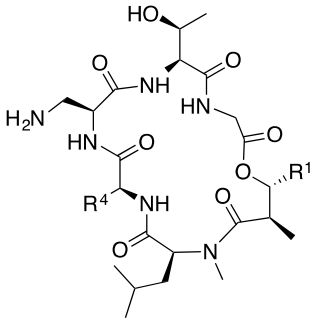

Compound	R^4	R^1	CFT073*imp*4213[a] MIC (μM)	CFT073[a] MIC (μM)	USA300[b] MIC (μM)	LogD (pH 7.4)
19		$-(CH_2)_9CH_3$	0.011	2.1	15	4.6
20		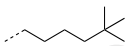	0.035	3.1	100	3.0
21		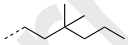	0.034	3.1	100	3.2
22		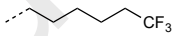	0.39	25	>100	2.0
23		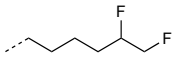	0.39	25	>100	1.6
24		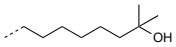	0.55	15	>100	2.2
25		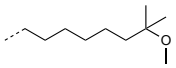	0.048	2.2	>100	2.8

[a] *E. coli*; [b] *S. aureus*

However, simply replacing the ester with the corresponding ether (**30**) reduced potency by only 3- fold and the resulting compound was also stable in plasma (Table 4). Ring enlargement (**31**) or substitution at the adjacent carbon (**32** and **33**) were not beneficial. Substitution at the β-carbon did provide a potency advantage, with the optimal stereochemistry providing compounds

35 a
affording excellent plasma stability.

We also attempted to replace the ester group with an amino linkage, and found that substantial activity was lost with compound **38** (Table 5). Interestingly, removing one carbon from the macrocyclic backbone, to generate an 18-membered ring instead of the 19-membered ring of globomycin, significantly improved activity, with **39** providing a MIC of 25 µM, and with no plasma stability issues. Within this context, the aliphatic tail can be placed at either position (**39** vs. **40**) or with two shorter aliphatic groups split between the two positions (**41**) all with similar activity. Similar to what was observed for the ether analogs, the introduction of a methyl group onto the backbone provided a few fold improvement in both OM-permeabilized and wild-type *E. coli* MICs as exemplified by compound **42**.

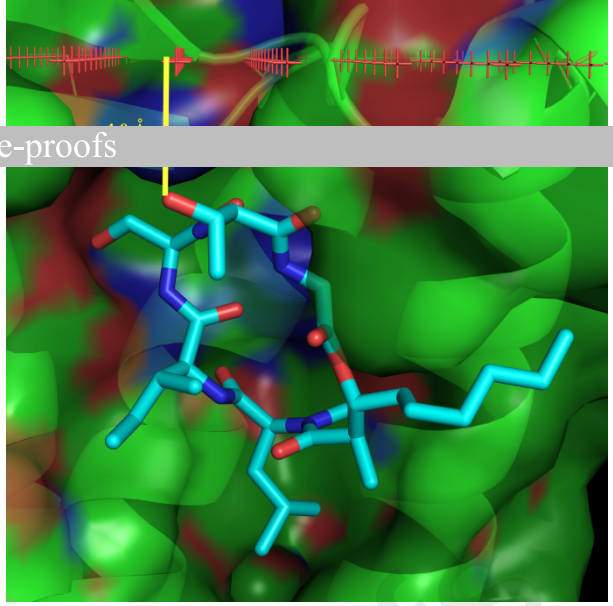

Figure 2: Distance from the allo-threonine globomycin side chain to the predicted membrane-periplasm interface (PDB 5DIR)

Table 3. Rigidified hydrophobic tails

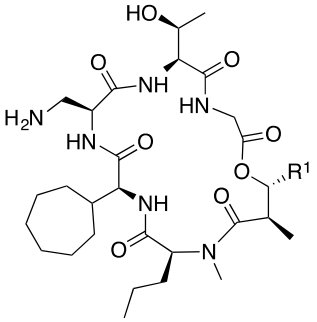

Compound	R¹	CFT073*imp*4213[a] MIC (µM)	CFT073[a] MIC (µM)	USA300[b] MIC (µM)	LogD (pH 7.4)
26[c]	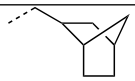	0.041	0.97	100	2.8
27[d]	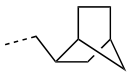	0.009	0.78	100	2.9
28	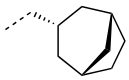	0.009	0.4	25	3.1
29		0.009	0.78	50	2.9

[a] *E. coli*; [b] *S. aureus;* [c]Mixture of exo diastereomers; [d]mixture of endo diastereomers

Tab

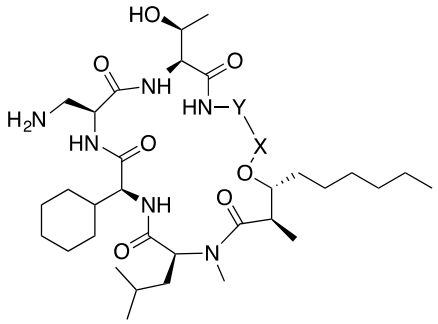

Compound	X	Y	CFT073*imp*4213 [a] MIC (μM)	CFT073[a] MIC (μM)	USA300[b] MIC (μM)	Plasma stability (h/m)
30	$-CH_2-$	$-CH_2-$	0.14	8.7	100	99% / 96%[c]
31	$-CH_2-$	$-CH_2CH_2-$	0.39	12	100	96% / 101%[d]
32	(*S*) $-CH(CH_3)-$	$-CH_2-$	0.1	12	100	91% / 101%[d]
33	(*R*) $-CH(CH_3)-$	$-CH_2-$	0.4	35	100	100% / 92%[d]
34	$-CH_2-$	(*S*) $-CH(CH_3)-$	1.0	84	71	88% / 93%[d]
35	$-CH_2-$	(*R*) $-CH(CH_3)-$	0.034	2.9	71	93% / 94%[d]
36 [e]	$-CH_2-$	(*R*) $-CH(CH_3)-$	0.048	4.4	100	100% / 91%[d]
37	$-CH_2-$	(*R*) $-CH(CH_2CH_3)-$	0.024	2.2	50	101% / 87%[d]

[a] *E. coli*; [b] *S. aureus*; [c] % parent remaining after 6 hour or [d] 24 hour incubation in either human (h) or mouse (m) plasma; [e] *N*-Me-norvaline instead of *N*-Me-leucine

s in Tables 4 and 5 are described in Schemes 3 and 4. Cyclic sulfamates could be used to alkylate a hydroxy acid to generate the corresponding alkoxy ester. Ester hydrolysis and an exchange of Boc for Fmoc protecting groups afforded the *N*-Fmoc-protected amino acids for peptide synthesis. Coupling to resin-bound tetra-peptides, Fmoc deprotection, and cleavage from the resin afforded linear amino acids, which were cyclized using HATU coupling followed by global side chain deprotection to afford the ether-linked macrocycles. Amino-linked macrocycles were prepared starting with benzyl or methyl ester protected amino acids, with two sequential reductive amination reactions providing the tertiary amines. Deprotection of the carboxylic acid and an exchange of Boc for Fmoc protecting groups afforded *N*-Fmoc-protected amino acids for peptide synthesis. Coupling to resin-bound tetra-peptides, Fmoc deprotection, and cleavage from the resin afforded linear amino acids, which were cyclized using HATU coupling

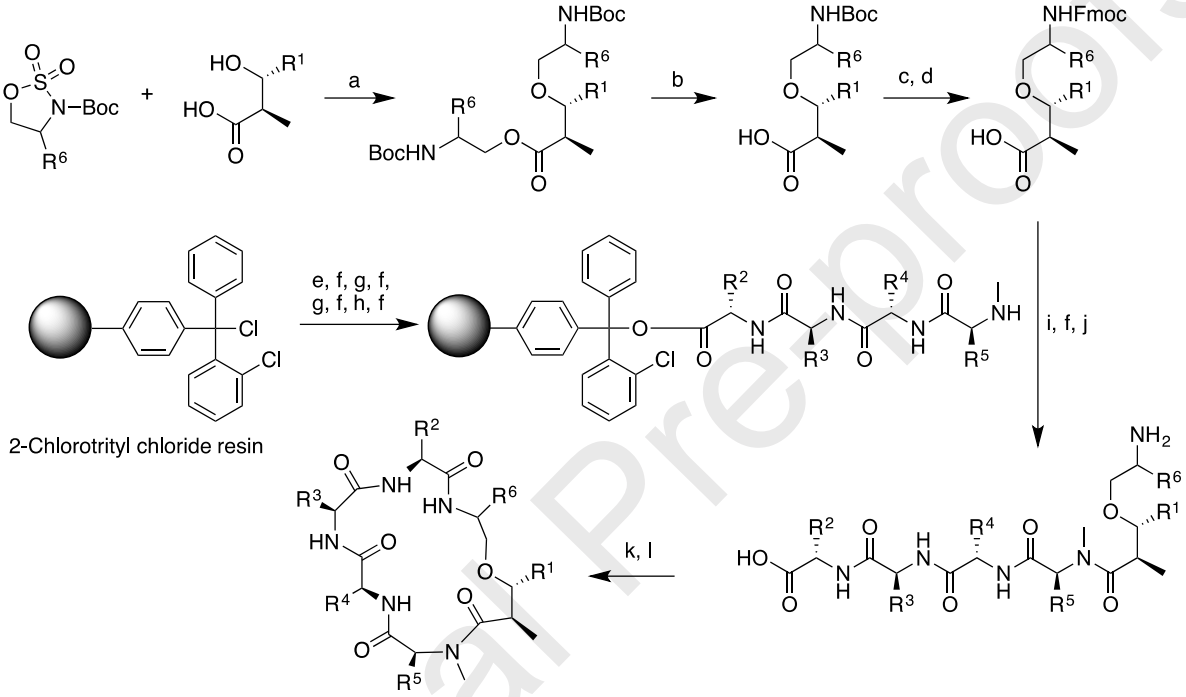

followed by global side chain deprotection to afford the amino-linked macrocycles. With plasma-stable compounds in hand, we evaluated the in vivo profile of **36** and **42**. Both compounds have low to moderate CL in rat liver microsomes and hepatocytes, but high CL was still observed when dosed IV in rats (Table 6). The increased CL observed in vivo relative to in vitro systems may be due to a combination of active hepatic uptake and passive renal filtration. The intrinsic permeability of these compounds is quite low (**36** MDCK Papp = 0.02 x10^{-6} cm/sec), and thus they may not be able to overcome any active transport mechanisms with passive permeability. (a) NaH, TBAF, THF; (b) LiOH, MeOH, H_2O; (c) HCl, dioxane; (d) Fmoc-Cl, LiOH, THF; (e) *N*-Fmoc amino acid, DIPEA, DMF; (f) piperidine, DMF; (g) *N*-Fmoc amino acid, DIPEA, HOBt, DMF; (h) *N*-methyl-*N*-Fmoc-protected

Scheme 3. Reagents and conditions: (a) NaH, TBAF, THF; (b) LiOH, MeOH, H_2O; (c) HCl, dioxane; (d) Fmoc-Cl, LiOH, THF; (e) *N*-Fmoc amino acid, DIPEA, DMF; (f) piperidine, DMF; (g) *N*-Fmoc amino acid, DIPEA, HOBt, DMF; (h) *N*-methyl-*N*-Fmoc-protected

physicochemical properties of a scaffold can affect transporter recognition. Globomycin scaffold SAR to this point indicated a fairly restricted chemical space seemingly without possibilities for adding additional polar or charged functionality. However, when the co-crystal structure of globomycin and LspA was analyzed to predict the boundaries of the membrane in which LspA would be embedded, the hydroxyl of the *allo*-threonine side chain is within 4 Å of the calculated IM-periplasm interface (Figure 2).[22] We hypothesized that a positively charged group may provide a favorable interaction with the negatively charged phosphate head groups at the periplasmic border of the lipid bilayer. Multiple positive charges are a common feature among antibiotics with gram negative activity, and may also enhance the ability of compounds to penetrate the OM.[23]

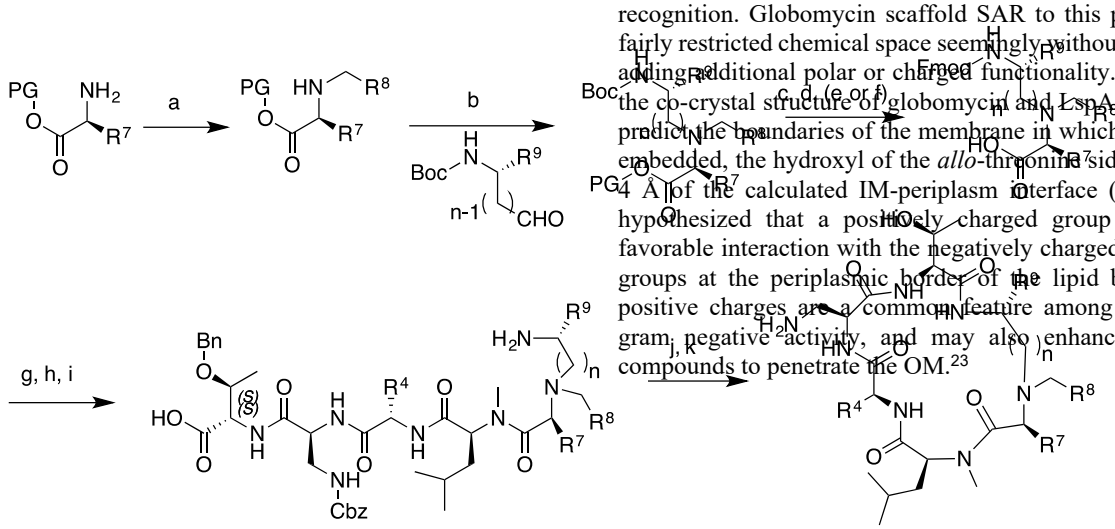

ami ion: TFA or Pd-C/H_2/EtOAc

Scheme 4. PG = Bn or CH_3. Reagents and conditions: (a) R^8-CHO, $NaBH(OAc)_3$, DCM or EtOAc; (b) $NaBH(OAc)_3$, DCM or EtOAc; (c) HCl, dioxane; (d) Fmoc-Cl, $NaHCO_3$; (e) LiOH, H_2O, THF; (f) Pd-C, H_2; (g) resin-bound tetrapeptide, DIPEA, HATU or PyAOP, DMF; (h) piperidine, DMF; (i) HFIP/DCM; (j) HATU, DIPEA, THF; (k) Pd-C/H_2

Consequently, we prepared a series of analogs with positively charged moieties at this position, following the general synthetic method described in Scheme 3. Analogs illustrated in Table 7 demonstrate the feasibility of this approach, with multiple compounds providing <10 μM MICs against wild type *E. coli*. There is flexibility in the structure of the linker, with both 3-carbon and 4-carbon linked amino groups providing similar activity (compounds **43** and **44**), and the corresponding tertiary amine **45** only marginally less active. Interestingly, the guanidine **46** had activity similar to the primary amine, but undesired *S. aureus* USA300 activity was increased. Aromatic rings could be included in the linker, as either a benzyl amine (**47**) or phenethylamine (**48**) led to 2- and 7-fold improvement in wild-type MIC vs **43**, respectively. Moving the ether oxygen farther from the core macrocycle provided a similar profile (**49** vs **50**). Adding small aliphatic rings (**51**) or a second charged amino group (**52** and **53**) to the linker provided some benefit in wild type *E. coli* compared to compound **43**. A carboxylic acid resulted in loss of activity against wild type *E. coli*, even with a positively charged spacer between the anion and the core macrocycle (compound **54**). The side-chain ether could be replaced with an amino, urea, or amide spacer with similar activity (compounds **56** – **58** compared to **55**).

Table 5. Macrocyclic amines

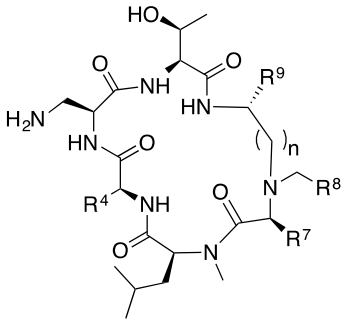

Compound	R^4	n	R^7	R^8	R^9	CFT073*imp*4213[a] MIC (μM)	CFT073[a] MIC (μM)	USA300[b] MIC (μM)	Plasma stability (h/m)[c]
38		2	CH3	$-(CH_2)_4CH_3$	H	12.5	>100	>100	101% / 100%
39		1	CH3	$-(CH_2)_4CH_3$	H	0.5	25	>100	95% / 112%
40		1	$-(CH_2)_5CH_3$	H	H	0.39	12	100	92% / 81%
41		1	$-(CH_2)_3CH_3$	$-(CH_2)_2CH_3$	H	0.1	6.3	100	ND[d]
42		1	$-(CH_2)_3CH_3$	$-(CH_2)_2CH_3$	CH3	0.017	1.6	71	97% / 89%

[a] *E. coli*; [b] *S. aureus*; [c]% parent remaining after 24 hour incubation in either human (h) or mouse (m) plasma; [d] ND = not determined

Table 6. Pharmacokinetic parameters for selected LspA inhibitors

Compound	LogD pH 7.4	Plasma stability (h/r/m)[a]	rat/mouse PPB (%)	RLM/MLM[b] (mL/min/kg)	Rat CL (mL/min/kg)	Rat $T_{1/2}$ (h)	Mouse CL (mL/min/kg)	Mouse $T_{1/2}$ (h)
globomycin	3.1	100% / 1% / 2%	NS / NS[c]	37 / 81			286	0.3
36	2.8	100% / 101% / 91%	97.1 / 98.5	20 / 69	148	0.3		
42	3.4	97% / 102% / 89%	99.5 / 99.6	27 / 77	53	2.6		
51	1.6	98% / 96% / 101%	96.7 / 98.9	20 / 43			2.9	4.0
59	2.2	103% / 90% / 84%	97.8 / 99.3	28 / 48	40	3.2	11	4.0
60	0.7	103% / 118% / 106%	97.5 / 99.9	ND / 53			12	4.6
61	1.7	99% / 94% / 95%	97.4 / 99.7	21 / 41	15	5.8	17	2.1
62	0.2	ND[c]	97.4 / 99.6	ND / ND			68	2.5
63	1.5	105% / 58% / 55%	95.3 / 97.4	<6.1 / 32	24	6.8		

[a]% parent remaining after 24 hour incubation in either human (h), rat (r), or mouse (m) plasma; [b] RLM = rat liver microsomes, MLM = mouse liver microsomes; [c] NS = not stable, ND = not determined

Table 7. Polar side chain SAR

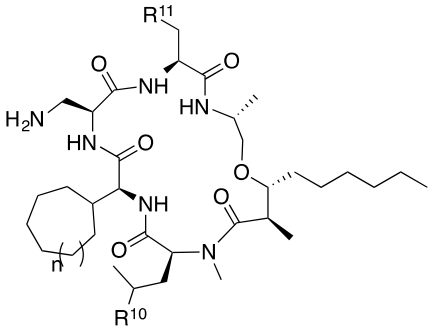

Compound	n	R^{10}	R^{11}	CFT073*imp* 4213[a] MIC (μM)	CFT073[a] MIC (μM)	USA300[b] MIC (μM)	LogD pH 7.4
43	0	CH_3	$-O-(CH_2)_3-NH_2$	0.28	11	100	1.5
44	0	CH_3	$-O-(CH_2)_4-NH_2$	0.18	7	56	1.7
45	0	CH_3	$-O-(CH_2)_3-N(CH_3)_2$	0.39	25	100	2.1
46	0	CH_3	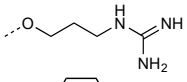	0.2	4.4	5	2.0
47	0	CH_3	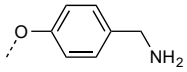	0.39	6.3	100	2.5
48	0	CH_3	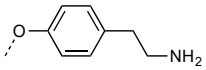	0.048	1.6	25	2.4
49	1	H	$-O-(CH_2)_4-NH_2$	0.14	6.3	71	1.8
50	1	H	$-CH_2-O-(CH_2)_3-NH_2$	0.2	8.8	100	1.7
51	1	H	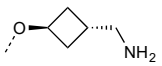	0.048	3.1	50	1.6
52	1	H	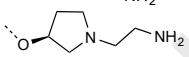	0.2	6.3	100	1.6
53	1	H	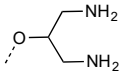	0.55	3.1	50	1.1
54	1	H	$-O-(CH_2)_3-NH-(CH_2)_3-CO_2H$	0.78	100	>100	1.3
55	1	H	$-NH-(CH_2)_3-NH_2$	0.28	3.1	50	1.1
56	1	H	$-N(CH_3)(CH_2)_3-NH_2$	0.39	8.8	100	1.8
57	1	H	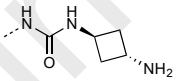	0.39	12	71	1.5
58	1	H	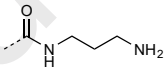	0.39	18	100	1.3

[a] *E. coli*; [b] *S. aureus*;

Interestingly, while the compounds in Table 7 generally maintained the wild-type MIC of parent compound **36**, the OM-permeabilized MIC was elevated, with the exception of compounds **48** and **51**. It is possible that analogs with a charged amine at this position reduced the intrinsic affinity of the inhibitor for LspA or hindered ability of the inhibitor to access the membrane-buried active site, resulting in decreased potency vs. the OM-permeabilized strain. At the same time, the overall physicochemical properties may enable better OM penetration and access to the target, with a resulting decrease in shift between OM-permeabilized and wild-type MICs. Selected compounds were tested in a *tolC*-deficient *E.coli* strain and showed a small shift in MIC, suggesting that reduction in efflux may also play a role (Supplementary Table S1). Optimized inhibitors containing both a charged sidechain and preferred rigidified lipophilic tails were prepared and are illustrated in Figure 3 (compounds **59** – **64**). Compared to globomycin itself, these inhibitors not only provide significant improvements in potency against *E. coli*, but also other *Enterobacteriaceae* and non-fermenter *P. aeruginosa* and *A. baumanii* strains, particularly compounds **59**, **60**, and **62** (Table 8). While these compounds do show measurable activity against *S. aureus* USA300, they do not inhibit the growth of a human Jurkat cell line, and so are unlikely to be generally cytotoxic. We also demonstrated that these compounds were specific to LspA as they show reduced growth inhibition of CFT073 strains that either were deficient in *lpp* or have over-expressed LspA, consistent with the previously published activity of globomycin (Supplementary Table S5).

In general, compounds **51** and **59-64** are moderately metabolized in rat and mouse liver microsomes, and have good

plas optimized inhibitors, and were pleased to see that compared to compounds **36** and **42**, these +2 or +3 charged inhibitors were able to achieve moderate or low CL in both mouse and rat IV studies generally overpredicted the measured in vivo CL, potentially due to the poor penetration of inhibitors into liver cells. still

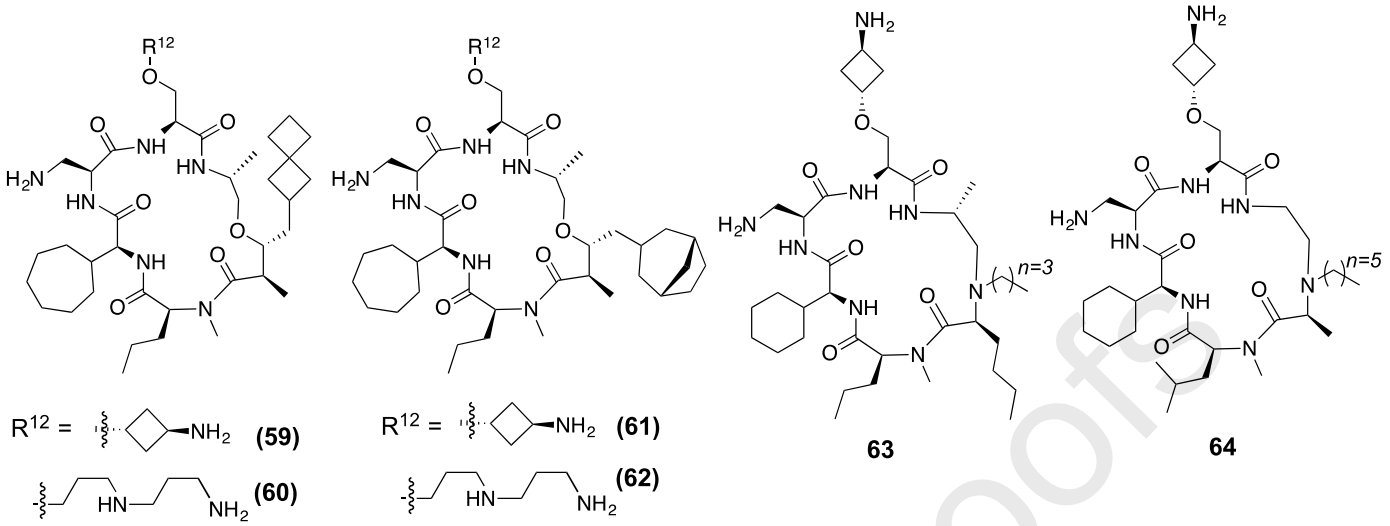

Figure 3. Optimized LspA inhibitors

Table 8. Optimized compounds demonstrate broad spectrum gram-negative activity

Compound	*E. coli* CFT073 MIC (μM)	*E. cloacae* MIC (μM)	*K. pneumoniae* MIC (μM)	*P. aeruginosa* MIC (μM)	*A. baumanii* MIC (μM)	*S. aureus* USA300 MIC (μM)	Cytotoxicity EC_{50} (μM)[a]
globomycin	44	100	>100	>100	>100	>100	>50
51	3.1	6.3	18	100	18	50	>100
59	2.2	6.3	8.8	71	18	25	ND
60	1.6	3.1	3.1	50	50	18	>50
61	0.78	3.1	8.8	100	25	50	>100
62	0.78	1.6	1.6	12	25	12	>100
63	6.3	ND	25	100	25	50	ND
64	6.3	ND	100	>100	>100	100	>100

[a]antiproliferative EC_{50} in a Jurkat cell growth assay

Based on observed low CL in mouse, compound **51** was advanced to a mouse neutropenic thigh model (*E. coli* 25922). Over a 20 hour IV infusion, an average blood concentration of 27 μM of compound **51** was reached, but no reduction in CFU was observed relative to vehicle treated animals. This is perhaps unsurprising since the free fraction of **51** in mouse plasma is only 1.1%, and the unbound concentration of compound (0.3 μM) is below the in vitro MIC for the *E. coli* 25922 strain (3.1 μM). Unfortunately, a higher dose of **51** was not tolerated and we were unable to evaluate the efficacy of an inhibitor where unbound exposures were commensurate with the in vitro MIC. The mechanism of toxicity observed at higher doses is unknown. Further improvements in MIC may be required to evaluate the in vivo efficacy of LspA inhibition.

In conclusion, the natural product globomycin was optimized to improve activity against wild-type *E. coli*, informed by the published co-crystal structure with LspA. While there are polar residues in the bottom of the active site that interact with backbone amides in the globomycin scaffold, we found that the overall lipophilic environment restricted options for optimization. Aside from a productive salt-bridge that was created with the catalytic aspartate residues, improvements in specific interactions with the protein remained elusive. Through replacement of the ester functionality, and through modification of physicochemical properties with the inclusion of an additional charged residue, we were able to obtain potent compounds with good in vivo PK properties. Optimized compounds demonstrate broad spectrum activity against Gram-negative bacterial pathogens. Despite the significant improvements in activity and in vivo stability, we were unable to achieve free concentrations in mice sufficient to demonstrate in vivo efficacy of LspA inhibition. We anticipate that optimization of this scaffold to achieve further improvements in activity and metabolic stability will enable us to demonstrate the promise of LspA inhibition as a new mode of action against Gram-negative bacteria.

Declaration of Competing Interest

Authors H.P., M-G.B., D.J.B., G.M.C., Y-C.C, J.C., G.D, S.L., R.P., C.S., M.X., Y.X., H.Z. S.B.K, and E.J.H. are employees of Genentech, Inc.

Acknowledgments

We gratefully acknowledge the Genentech and Pharmaron analytical chemistry groups as a whole, and Won Choi and Kewei

purification and purity analysis. We thank Zhengyin Yan for advice and discussion on DMPK methods.

Supplementary Material

Supplementary data associated with this article can be found online at XXX and includes: Supplementary Tables S1 through S5; experimental methods describing determination of MICs, plasma protein binding, plasma stability, liver microsome and hepatocyte stability, MDCK permeability, and LogD; analytical data, purity determination, and synthetic methods for lead compounds.

References and notes

1. Ventola, C. L. The Antibiotic Resistance Crisis: Part 1: Causes and Threats. *P. T.* **2015**, *40* (4), 277–283.
2. Arnaout, El, T.; Soulimane, T. Targeting Lipoprotein Biogenesis: Considerations Towards Antimicrobials. *Trends in Biochemical Sciences* **2019**, 1–15.
3. Xia, J.; Feng, B.; Wen, G.; Xue, W.; Ma, G.; Zhang, H.; Wu, S. Bacterial Lipoprotein Biosynthetic Pathway as a Potential Target for Structure-Based Design of Antibacterial Agents. *CMC* **2019**, *26*, 1–18.
4. Tokunaga, M; Tokunaga, H; Wu, H.C.; Post-translational modification and processing of Escherichia coli prolipoprotein in vitro. Proc Natl Acad Sci USA **1982**, *79*, 2255–2259.
5. Zwiebel, L. J.; Inukai, M.; Nakamura, K.; Inouye, M. Preferential Selection of Deletion Mutations of the Outer Membrane Lipoprotein Gene of Escherichia Coli by Globomycin. *J. Bacteriol.* **1981**, *145* (1), 654–656.
6. Hussain, M.; Ichihara, S.; Mizushima, S. Accumulation of glyceride-containing precursor of the outer membrane lipoprotein in the cytoplasmic membrane of Escherichia coli treated with globomycin. *J. Biol. Chem.* **1980**, *255*, 3707-3712.
7. Inukai, M.; Takeuchi, M.; Shimizu, K.; Arai, M. Mechanism of Action of Globomycin. *J. Antibiotics* **1978**, *31* (11), 1203–1205.
8. Xiao, Y.; Gerth, K.; Müller, R.; Wall, D. Myxobacterium-Produced Antibiotic TA (Myxovirescin) Inhibits Type II Signal Peptidase. *Antimicrob Agents Chemother* **2012**, *56* (4), 2014–2021.
9. Inukai, M.; Nakajima, M.; Osawa, M.; Haneishi, T.; Arai, M. Globomycin, a New Peptide Antibiotic with Spheroplast-Forming Activity. II. Isolation and Physico-Chemical and Biological Characterization. *J. Antibiotics* **1978**, *31* (5), 421-425.
10. Nakajima, M.; Inukai, M.; Haneishi, T.; Terahara, A.; Arai, M.; Kinoshita, T.; Tamura, C. Globomycin, a New Peptide Antibiotic with Spheroplast-Forming Activity. III. Structural Determination of Globomycin. *J. Antibiotics* **1978**, *31* (5), 426-432.
11. Kitamura, S.; Owensby, A.; Wall, D.; Wolan, D. W. Lipoprotein Signal Peptidase Inhibitors with Antibiotic Properties Identified **2018**, 1–21.
12. Kiho, T.; Nakayama, M.; Yasuda, K.; Miyakoshi, S.; Inukai, M.; Kogen, H. Synthesis and Antimicrobial Activity of Novel Globomycin Analogues. *Bioorg. Med. Chem. Lett.* **2003**, *13* (14), 2315–2318.
13. Kiho, T.; Nakayama, M.; Yasuda, K.; Miyakoshi, S.; Inukai, M.; Kogen, H. Structure–Activity Relationships of Globomycin Analogues as Antibiotics. *Bioorg. Med. Chem.* **2004**, *12* (2), 337–361.
14. Vogeley, L.; Arnaout, El, T.; Bailey, J.; Stansfeld, P. J.; Boland, C.; Caffrey, M. Structural Basis of Lipoprotein Signal Peptidase II Action and Inhibition by the Antibiotic Globomycin. *Science* **2016**, *351* (6275), 876–880.
15. Zgurskaya, H. I.; López, C. A.; Gnanakaran, S. Permeability Barrier of Gram-Negative Cell Envelopes and Approaches to Bypass It. *ACS Infect. Diseases* **2015**, *1* (11), 512–522.
16. Stoll, H.; Dengjel, J.; Nerz, C.; Götz, F. *Staphylococcus Aureus* Deficient in Lipidation of Prelipoproteins Is Attenuated in Growth and Immune Activation. *Infect. Immun.* **2005**, *73* (4), 2411–2423.
17. Kogen, H.; Kiho, T.; Nakayama, M.; Furukawa, Y.; Kinoshita, T.; Inukai, M. Crystal Structure and Total Synthesis of Globomycin: Establishment of Relative and Absolute Configurations. *J. Am. Chem. Soc.* **2000**, *122* (41), 10214–10215.
18. Sarabia, F.; Chammaa, S.; García-Ruiz, C. Solid Phase Synthesis of Globomycin and SF-1902 a 5. *J. Org. Chem.* **2011**, *76* (7), 2132–2144.
19. Oppolzer, W.; Lienard, P. Efficient Asymmetric Synthesis of Anti-Aldols From Bornanesultam Derived Boryl Enolates. *Tett. Lett.* **1993**, *34*, 4321–4324.
20. Thern, B.; Rudolph, J.; Jung, G. Triphosgene as Highly Efficient Reagent for the Solid-Phase Coupling of N-Alkylated Amino Acids—Total Synthesis of Cyclosporin O. *Tet. Lett.* **2002**, *43*, 5013–5016.
21. Shiina, I.; Fukui, H.; Sasaki, A. Synthesis of Lactones Using Substituted Benzoic Anhydride as a Coupling Reagent. *Nat. Protoc.* **2007**, *2* (10), 2312–2317.
22. Lomize, M. A.; Pogozheva, I. D.; Joo, H.; Mosberg, H. I.; Lomize, A. L. OPM Database and PPM Web Server: Resources for Positioning of Proteins in Membranes. *Nucleic Acids Res.* **2012**, *40* (Database issue), D370–D376.
23. Brown, D. G.; May-Dracka, T. L.; Gagnon, M. M.; Tommasi, R. Trends and Exceptions of Physical Properties on Antibacterial Activity for Gram-Positive and Gram-Negative Pathogens. *J. Med. Chem.* **2014**, *57* (23), 10144–10161.